Pre-mutagenic and mutagenic changes imprinted on the genomes of mammalian cells after irradiation with a nail polish dryer

Maria Zhivagui[1,2,3], Noelia Valenzuela[3], Yi-Yu Yeh[2], Jason Dai[2], Yudou He[1,2,3], and Ludmil B. Alexandrov[1,2,3*]

Affiliations

[1]Department of Cellular and Molecular Medicine, UC San Diego, La Jolla, CA, 92093, USA

[2]Department of Bioengineering, UC San Diego, La Jolla, CA, 92093, USA

[3]Moores Cancer Center, UC San Diego, La Jolla, CA, 92037, USA

[*]Correspondence should be addressed to L2alexandrov@health.ucsd.edu.

ABSTRACT

Ultraviolet A light (UVA) is commonly emitted by nail polish dryers with recent reports suggesting that long-term use of UV-nail polish dryers may increase the risk for developing skin cancer. However, no experimental evaluation has been conducted to reveal the effect of radiation emitted by UV-nail polish dryers on mammalian cells. Here, we examine the pre-mutagenic and mutagenic changes imprinted on the genomes of human and murine primary cell models due to irradiation by a UV-nail dryer. Our findings demonstrate that radiation from UV-nail devices is cytotoxic and genotoxic. Importantly, high levels of reactive oxygen species were observed in all irradiated samples. Analysis of somatic mutations revealed a dose-dependent increase of C:G>A:T substitutions in irradiated samples with a pattern consistent to the one of COSMIC signature 18, a mutational signature attributed to reactive oxygen species. Examination of previously generated skin cancer genomics data revealed that signature 18 is ubiquitously present in melanoma and that it accounts for ~12% of the observed driver mutations. In summary, this study demonstrates that radiation emitted by UV-nail polish dryers can both damage DNA and can permanently imprint somatic mutations on the genomes of mammalian cells. These results have far reaching implications in regard to public health and to preventing skin cancer due to occupational- or consumer-based exposure to ultraviolet light from artificial sources.

INTRODUCTION

Ultraviolet (UV) light is a type of electromagnetic radiation that has a wavelength ranging between 10nm and 400nm. Since wavelengths below 280nm are generally blocked by the Earth's stratospheric ozone, the UV light that reaches the Earth's surface is between 280nm and 400nm[1]. This spectrum can be further categorized based on its effect on human skin. Ultraviolet B light (UVB; 280-315nm) accounts for about 10% of the UV found on Earth, it penetrates the outer layer of the skin, and it induces a plethora of DNA lesions including cyclobutane-pyrimidine dimers and 6-4 photoproducts[2]. In contrast, ultraviolet A light (UVA; 315-400nm) constitutes approximately 90% of the ultraviolet radiation that reaches the surface of the Earth, it can penetrate the skin more deeply, and it causes little direct DNA damage as UVA is poorly absorbed by DNA[3].

The International Agency for Research on Cancer has classified UVA as a Group 1 carcinogen, based on sufficient evidence for carcinogenicity in both humans and experimental models combined with strong mechanistic considerations[4]. Importantly, this classification as well as the majority of prior research has utilized broadband UVA radiation (315-400nm) while many consumer products emit radiation only in a small subset of this spectrum (most above 360nm). Consistent with IARC's classification, meta-analyses have shown a causal relation between skin cancer and irradiation with UV-emitting tanning devices[4,5]. Similarly, it has been demonstrated that skin squamous-cell carcinoma developed in mice with long-term exposure to broadband UVA[6-9]. Prior experimental studies have suggested that UVA irradiation leads to indirect DNA damage mostly through the accumulation of 8-oxo-7,8-dihydroguanine derived from reactive oxygen species[10-14]. Studies using reporter single-gene assays have identified an enrichment of C:G>A:T mutations in UVA irradiated samples consistent with damage due to 8-oxo-7,8-

dihydroguanine[15-18]. Despite prior evidence for carcinogenicity of broadband UVA (315-400nm), UVA radiation in subsets of this spectrum is widely used in a surfeit of consumer products without extensive evaluation of the potential carcinogenic and mutagenic effects of these products. One prominent example is UV-nail polish dryers, which have become increasingly popular in the last decade[19,20].

UV-nail lamps are used to cure and dry nail polish formulas, known as gels, which are oligomers requiring exposure to UV radiation to harden into polymers. These UV-gel nail devices release UVA radiation with either very little or, in most cases, no UVB radiation[21]. UV-gel nail devices contain multiple bulbs, emitting UV wavelengths between 340 and 395nm that can react and activate the photo-initiators in the gel[19]. Concerns have been raised regarding the magnitude of DNA damage that can be posed from exposure to UV-nail machines and their potential role in skin carcinogenesis[20,22]. Notably, in most cases, both nails and hands are irradiated up to 10 minutes with a UV-nail dryer per session[22]. The number of nail salon clients is estimated to reach 8 clients a day per nail technician, accounting for approximately 3 million daily clients in the United States[23]. Typically, regular consumers change their gel manicures every 2 weeks[22]. Recently, a small number of melanoma and non-melanoma cases, reported either on the nail or on the dorsum of the hand, have been putatively attributed to exposure to UV radiation emitted by nail polish dryers[22,24].

To evaluate the pre-mutagenic and mutagenic effects of ultraviolet radiation emitted by nail polish UV-dryers on mammalian cells, we performed an *in vitro* irradiation of human and murine primary cells using distinct acute and chronic exposure protocols. Irradiated and control cells were

subjected to multiple assays for measuring DNA damage as well as to whole-genome sequencing after clonal expansion (**Figure 1**). Comparison between irradiated and control cells demonstrated that radiation (365-395nm) from a UV-nail dryer induces cytotoxicity, genotoxicity, and mutagenicity in a dose-dependent manner. Reactive oxygen species were highly elevated in irradiated samples and a mutational signature, previously attributed to reactive oxygen species[25,26], was found imprinted on the genomes of irradiated samples. Patterns of mutations consistent with cyclobutane pyrimidine dimers or 6–4 photoproducts were not observed in any of the irradiated sample. In summary, our analysis uncovers both the spectrum of pre-mutagenic lesions and the mutational signatures engraved on the genomes of mammalian cells by ultraviolet radiation emitted by a UV-nail polish dryer. These results demonstrate that UV light emitted by artificial lamps can both damage mammalian DNA as well as permanently imprint somatic mutations on the genomes of these cells. Our findings have far reaching implications in regard to public health and in regard to preventing skin cancer due to occupational or consumer-based exposure to ultraviolet light.

RESULTS

Cytotoxicity of mammalian cells after irradiation by a UV-nail dryer

To study the effect of exposure to UV radiation generated by a UV-nail polish dryer, mouse embryonic fibroblasts (MEFs) and human foreskin fibroblasts (HFFs) were irradiated under several distinct conditions. Each primary cell line was irradiated either one, two, or three times, with the duration of each exposure lasting between 0 and 20 minutes. Further, each condition was repeated at least three times to account for any technical variability. Analysis of cell viability reveals that UV radiation induced cytotoxicity with higher number of exposures causing a lower cell viability (**Figure 2*A***). For example, a single 20-minute irradiation of MEFs resulted in ~23% cell death, while three consecutive 20-minute exposures caused approximately 65% cell death (p-value: 0.0033; Student's t-test; **Figure 2*A***). Irradiated HFFs showed similar behavior to the one exhibited by MEFs (**Figure 2*A***). For example, about 20% of HFFs died due to a single 20-minute exposure and ~68% cell death was observed when cells were exposed three times with each exposure lasting 20 minutes (p-value: 0.05; Student's t-test; **Figure 2*A***).

Pre-mutagenic and mutagenic analyses were performed on MEFs and HFFs after either two 20-minute irradiations taking place within 2 hours in a single day (termed, acute exposure; **Figure 1**) or after three 20-minute irradiations each occurring in 3 consecutive days (termed, chronic exposure; **Figure 1**). For both acute and chronic exposures, all subsequent experiments were performed after completion of the last irradiation.

Pre-mutagenic lesions in mammalian cells after irradiation by UV-nail dryer

Pre-mutagenic lesions in mammalian cells irradiated with a UV-nail polish dryer were evaluated using γH2Ax immunofluorescence for genotoxicity due to the induction of DNA double-strand breaks and with OxiSelect™ *in vitro* assay for the presence of cytosolic and extra-cellular reactive oxygen species (ROS). Genotoxicity and DNA breaks were determined 4 hours post-exposure, whereas ROS production was assessed in three different timepoints: immediately after exposure, 20 minutes post-irradiation, and 24 hours post-irradiation.

A significant increase in the number of γH2Ax foci was observed when comparing irradiated MEFs or HFFs to control cells for both acute and chronic exposures (**Figure 2*B***). For MEFs, the number of γH2Ax fluorescent cells increased to an average of 72% (q-value: 0.0031; Student's t-test) and 82% (q-value: 0.00027) of the total number of examined cells for acute and chronic exposures, respectively (**Figure 2*C***). Similarly, the average percentage of γH2Ax fluorescent cells was elevated to 50% for acutely exposed HFFs (q-value: 0.0052;) and 87% for chronically exposed HFFs (q-value: 0.0017; **Figure 2*C***).

In terms of ROS production, cytosolic and extra-cellular ROS were elevated in both acutely and chronically exposed mammalian cells compared to the untreated cells for most timepoints (**Figure 2*D***). For both HFFs and MEFs, acute exposure resulted in 2- to 8-fold increase of both cytosolic and extra-cellular ROS compared to their respective controls (q-values: 0.002 and 7.2×10^{-8} for HFF cytosolic and extracellular, respectively; 2.8×10^{-7} and 1.7×10^{-9} for MEF cytosolic and extracellular, respectively; Student's t-test). Interestingly, cytosolic ROS decreased within 24 hours in both cell types for acute and chronic exposures. This suggests that ROS is likely generated

intracellularly and, subsequently, possibly transferred to the outer layer of the cells. Similarly, ROS was also elevated in chronically exposed HFFs and MEFs as compared to their respective controls (q-values: 8.2×10^{-4} and 2.3×10^{-6} for HFF cytosolic and extracellular, respectively; 5.1×10^{-10} and 2.7×10^{-10} for MEF cytosolic and extracellular, respectively).

Mutations found in the genomes of mammalian cells irradiated by a UV-nail dryer

Exposure of murine cells to UV radiation from a nail dryer gave rise to multiple immortalized clones, emerging relatively faster than the clones from the spontaneous cultures (**Supplementary Figure 1*A***). In contrast, irradiated human cells underwent recovery phase post UV treatment and were amendable to single-cell clone formation at a later timepoint compared to the control cells (**Supplementary Figure 1*B***). Comparably, human irradiated cells led to *bona fide* clone formation relatively faster than the human spontaneous cultures. A total of 12 clones were subjected to whole-genome sequencing at 30x and compared to primary cells to derive somatic mutations (**Supplementary Figure 2**; **Supplementary Tables 1 & 2**). Specifically, we sequenced one acute UV-derived HFF clone, 3 HFF clones generated from chronic irradiation with the UV-nail dryer, 3 MEF clones from acutely irradiated cultures with a UV-nail dryer, and 3 MEF clones derived from chronic irradiation with a UV-nail dryer. Additionally, 2 spontaneous control clones, one HFF and one MEF, were also sequenced.

Single base substitutions (SBSs) were 2.7- and 1.4-fold elevated respectively in chronically and acutely irradiate MEF cells compared to control cells (q-values: 0.08 and 0.19*;* Student's t-test; **Figure 3*A***). Stratification of SBSs based on their simplest six channel classification (*i.e.*, C>A, C>G, C>T, T>A, T>C, T>G; each mutation referred to by the pyrimidine base of the Watson-

Crick DNA base-pair) revealed a significant increase of C>A transversions in chronic MEFs exposed to UV light emitted from a nail dryer: 4.2- and 1.7-fold increase for chronic and acute, respectively (q-values: 0.03 and 0.29; Student's t-test; **Figure 3*B***). An elevation of C>A mutations was also observed in acutely irradiated HFF clones (1.5-fold increase with q-value: 0.002 Student's t-test; **Figure 3*B***) but not in chronically irradiated HFF clones (1.1-fold increase with q-value: 0.50; **Figure 3*B***). Importantly, the number of C>A single base substitutions found in MEF clones was positively correlated with the number of UV exposures (**Figure 3*C***; Spearman correlation: 0.85; q-value*:* 0.016). No correlation was observed for any type of single base substitutions in HFFs (**Figure 3*C*** and **Supplementary Figure 3**). Additional analysis of the variant allele frequency (VAF) for single base substitutions revealed that the majority of HFF mutations are clonal with a mean VAF of approximately 0.50 while the majority of MEF mutations are subclonal with a mean VAF of approximately 0.25 (**Supplementary Figure 4*A & B***). Moreover, VAF data split into 3 bins indicated an enrichment of C>A mutations in high VAF (0.66 to 1) accounting for around 50% of all substitutions in both MEFs and HFFs (**Figure 3*F & G***). This increase was also maintained at medium and low VAF (medium: 0.33 to 0.66; low: 0 to 0.33), indicating a potential selection of cells harboring C>A mutations during clonal expansion. No differences were observed between irradiated and control cells in regard to small insertions and deletions (**Supplementary Figure 4*C***).

To evaluate any functional effect of the imprinted somatic mutations, we examined the non-synonymous mutations in irradiated clones. Non-synonymous mutations were found in 371 genes across all MEFs and in 77 genes across all HFFs with a wide range of VAFs (**Figure 4*A & B***). To evaluate the early events driving barrier bypass and immortalization, genes with heterozygous

197 mutations (VAF between 0.25 and 0.75) were compared to the most recent COSMIC cancer gene
198 census[27-32]. The comparison revealed 8 mutated cancer census genes in MEFs, including, *TP53*'s
199 mouse orthologue *Trp53*, and 9 mutated cancer census genes in HFFs. In MEFs, mapping mutated
200 genes to Gene Ontology (GO) enrichment analysis unearthed several significantly mutated
201 biological processes revolving around oxidative damage activity (namely, gene ontology terms
202 GO:0016705 and GO:0016712). Similarly, in HFFs, we observed a significant deregulation in
203 biological processes related to oxidative damage activity (namely, gene ontology terms
204 GO:0016645 and GO:0016811).
205
206 **Mutational signatures imprinted by irradiating with a UV-nail polish dryer**
207 Previously, we have shown that different endogenous and exogenous mutational processes imprint
208 characteristic patterns of somatic mutations, termed, mutational signatures[33-35]. To evaluate the
209 mutational signatures imprinted by irradiation with a UV-nail polish dryer, we first constructed
210 background mutational models based on the continuously ongoing clock-like mutational
211 signatures[36] and the mutational patterns observed in the spontaneous MEF and HFF clones,
212 respectively. To explain the SBS patterns of mutations observed in the irradiated MEF and HFF
213 cells, any known COSMIC signature[33] that improves the reconstruction above the background
214 model was allowed. For example, in one of the chronically exposed MEF clones, in addition to the
215 background mutational pattern, only COSMIC signature 18 was found allowing an overall
216 reconstruction with an accuracy of 0.94 (**Figure 5*A***); adding any other COSMIC signature would
217 improve the overall accuracy with no more than 0.0025 (or 0.25%). Similarly, COSMIC signature
218 18, a signature previously attributed to reactive oxygen species[25,26], was found to be operative in
219 5 of the 6 irradiated MEF and 2 of the 4 irradiated HFF cells, (**Figure 5*B* & Supplementary Table**

220 **1**). All irradiated samples without signature 18 had patterns of mutations similar to the one
221 observed in the spontaneous clone with only one of these samples exhibiting signature 2 at low
222 levels; no other mutational signatures were observed in any of the samples (**Supplementary Table**
223 **1**). For MEFs, chronically exposed cells harbored more signature 18 mutations than acutely
224 exposed cells (**Figure 5*B***). For HFFs, similar levels of signature 18 were observed in both the
225 chronic and acutely irradiated samples that exhibited signature 18 (**Figure 5*B***). Observing
226 signature 18, which is almost exclusively characterized by C>A substitutions, in irradiate clones
227 confirms that radiation from a UV-nail polish dryer not only oxidize DNA but that this oxidative
228 damage results in permanently imprinted mutations on the genomes of irradiated cells.
229
230 Re-examination of the recently published set of 107 whole-genome sequenced skin cancers from
231 the Pan-Cancer Analysis of Whole Genomes (PCAWG) project[37] revealed that an average skin
232 cancer harbors approximately 2,500 C>A substitutions (95% CI: 2,015 – 2,868) in their genome
233 with 93% of their pattern matching the one of signature 18. However, these C>A substitutions
234 account for only 2.16% of the mutations observed in the 107 melanomas; 85% of mutations in
235 these melanomas are generated by signature 7 – mutational signature attributed to cyclobutane-
236 pyrimidine dimers and 6-4 photoproducts due to ultraviolet light[38]. Importantly, 20 of the 169
237 substitutions (11.83%) identified as driver mutations[37] in these 107 samples can be attributed to
238 signature 18. This indicates that, while signature 18 generates low numbers of mutations in skin
239 cancer, it plays an important role in generating somatic mutations that contribute towards tumor
240 development and evolution.

DISCUSSION

In this report, we employed well-controlled experimental models for UV irradiation using a UV-nail polish dryer and evaluated the pre-mutagenic and mutagenic changes imprinted on the genomes of mammalian cells (**Figure 1**). The utilized *in vitro* clonal expansion models manifest the specific features required for mimicking human carcinogenesis and for recapitulating the activity of characteristic mutational processes[39]. Both MEFs and HFFs underwent clonal expansion after a barrier bypass step (senescence for MEFs and single-cell bottleneck for HFFs) leading to the formation of exposure-derived clones (**Supplementary Figure 1**). Cytotoxicity and genotoxicity were observed in all irradiated cultures; importantly, we observed at least 2-fold elevation of ROS in irradiated cells (**Figure 2**). Higher levels of somatic mutations were also observed in most of the irradiated clones and mutations were found in pathways known to be affected by reactive-oxygen species (**Figures 3 & 4**). Consistent with the increase of ROS, whole-genome sequencing revealed that COSMIC signature 18, a mutational signature previously attributed to reactive oxygen species[25,26], is imprinted on the genomes of irradiated samples (**Figure 5**).

Broadband UVA (315-420nm) has been extensively studied in the context of tanning devices and classified as carcinogen by the International Agency for Research on Cancer[4]. Prior experimental studies with broadband UVA have shown that it causes an accumulation of 8-oxo-7,8-dihydroguanine[10-14], generates C>A mutations in single-gene assays[15-18], and even induces tumors in mice[40]. Indeed, prior studies have shown that UVA can generate low level of C>T somatic mutations consistent with pyrimidine-pyrimidine photodimers[41]. Intriguingly, in this study, we demonstrate that UVA with wavelengths between 365 and 395nm, which is generally considered

to be safe and is commonly used in a plethora of consumer products, causes DNA oxidation and C>A mutations on a genomic scale with some mutations appearing in known cancer driver genes; no evidence was found that the radiation generated by the UV-nail polish machine generates any pyrimidine-pyrimidine photodimers.

Our findings are also consistent with prior cancer epidemiological observations. In principle, males have significantly higher risk than females to develop melanoma[42,43]. Surprisingly, this trend is reversed when one examines cancer risk in melanomas of the hand in younger women. Specifically, young females (ages 15 to 39) have approximately 2-fold higher risk for developing melanoma of the upper extremities compared to young males[44]. This higher risk is possibly due to lifestyle choices, one of which may be radiation from female-focused consumer products such as UV-nail polish dryers[44]. It should be noted that exposure to UV-light from the sun cannot reasonably explain the higher risk in young females as there is no observed differences in melanoma risk between young males and females for other parts of the body commonly exposed to the sunlight, *viz.*, face, head, and neck[43,44].

While this report demonstrates that radiation from UV-nail polish dryers is cytotoxic, genotoxic, and mutagenic, it does not provide direct evidence for increased cancer risk in human beings. Prior studies have shown that an increase in mutagenesis can correspond to an increase in cancer risk[45-47]. Further, several anecdotal cases have demonstrated that cancers of the hand can be due to radiation from UV-nail polish dryers[22,24]. Taken together, our experimental results and the prior evidence strongly suggest that radiation emitted by UV-nail polish dryers may cause cancers of the hand and that UV-nail polish dryers, similar to tanning beds[48], may increase in the risk of early-

287 onset skin cancer[49]. Nevertheless, future large-scale epidemiological studies are warranted to
288 accurately quantify the risk for skin cancer of the hand in people regularly using UV-nail polish
289 dryers. It is likely that such studies will take at least a decade to complete and to subsequently
290 inform the general public. In the meantime, this report aims to raise awareness of the likely cancer-
291 causing role of artificial UV lamps and caution people who regularly use UV-nail polish dryers.

MATERIALS AND METHODS

UV-nail polish machine characteristics

A 54-Watt UV nail drying machine was purchased (model: MelodySusie), harboring 6 bulbs that emit UV photons for curing gel nail polishes. Based on the manufacturer's specifications, the UV nail drying machine emits ultraviolet A light in wavelengths between 365 and 395nm. The UV power density was measured using a UV513AB Digital UVA/UVB Meter that can measure UV radiation between 280 and 400 nm. The machine stabilizes at ~7.5 mW/cm^2, within minutes (**Supplementary Figure 5*A* & *B*),** putting it on the lower end of the power density spectrum calculated for commonly used UV-nail machines[21] (median of 10.6 mW/cm^2). In this study, in most cases, we performed a 20-minute UV exposure session which is equivalent to a total amount of energy delivered per unit area of 9 J/cm^2:

$$7.5\ mW/cm^2 * 20\ minutes = 7.5\ mJ/(sec*cm^2) * 1200\ sec = 9000\ mJ/cm^2 = 9\ J/cm^2$$

Cell culture, exposure and immortalization of mouse embryonic fibroblasts (MEFs)

Primary mouse embryonic fibroblasts (MEFs) were expanded in Advanced DMEM supplemented with 15% fetal bovine serum, 1% penicillin/streptomycin, 1% sodium pyruvate and 1% glutamine, and incubated in 20% O_2 and 5% CO_2. At passage 2, the primary cells were seeded in six-well plates for 24 hours, until adherence, then exposed for 20 minutes to the UV-nail machine in pre-warmed sterile PBS. Control cells were kept in PBS for 20 minutes. The cells were exposed to UV, acutely (*i.e.*, twice a day, with 60 minutes break between the 2 sessions) and chronically (*i.e.*, once every day for up to 3 consecutive days). At the end of every UV treatment, the cells were washed, and complete pre-warmed medium is replenished. Exposed and control primary cells were

315 cultivated until bypassed a barrier step, namely senescence in MEFs and single-cell subcloning
316 using serial dilutions technic in HFFs. Upon barrier bypass, the cells reached clonal expansion
317 allowing the isolation of *bona fide* cell clones. All cell cultures were routinely tested for the
318 absence of mycoplasma.
319
320 **Cell culture, exposure, and immortalization of human foreskin fibroblasts (HFFs)**
321 Primary human cells derived from human foreskin fibroblasts (HFFs) were provided to us by Dr.
322 John Murray (Indiana University Bloomington). Early passage cells were expanded in Advanced
323 DMEM supplemented with 10% fetal bovine serum and 1% glutamine in 5% CO_2 incubator.
324 Exposure to UV radiation followed same protocol as the one for MEFs. Clonal expansion was
325 carried out using serial dilutions procedure in 96-well plates, following calculations assuming 30%
326 probability of a single-cell clone formation per well. Wells were washed weekly, until clones
327 reached confluency and were transferred progressively to T-75 flasks. Thirteen single-cell clones
328 from 3 experimental replicates of UV chronic exposure and 8 clones in total for the control
329 untreated cells were successfully isolated.
330
331 **Cell viability and cytotoxicity assays**
332 Primary cells were seeded in 24-well plates and exposed to the UV drying device as indicated.
333 Cell viability was measured 48 hours after treatment cessation using the Cell-Counting Kit 8
334 (CCK-8) from Dojindo. Plates were incubated for 3 hours at 37°C and absorbance was measured
335 at 450 nm using the Infinite 200 Tecan *i*-control plate reader machine. The CCK-8 assay was
336 performed in 4 replicates for each experimental condition. Trypan Blue exclusion assay was also
337 performed for assessing cell viability upon exposure, validating the choice for selecting the

338 indicated UV exposure conditions inducing around 50% cell death (**Supplementary Figure 5*C***).
339 In addition, Trypan Blue assay was used to compute the doubling population of the cells in culture.
340

341 **γH2Ax Immunofluorescence for assessment of genotoxicity**

342 Immunofluorescence staining was carried out using a monoclonal antibody specific for Ser139-
343 phosphorylated H2Ax (γH2Ax) (9718, Cell Signaling Technology). Briefly, primary cells were
344 seeded on coverslips in 24-well plates and, the following day, exposed to UV radiation as
345 indicated, in duplicates. Four hours after treatment cessation, the cells were fixed with 4%
346 formaldehyde at room temperature (RT) for 15 minutes, followed by blocking in 5% normal goat
347 serum (5425, Life Technologies) for 60 minutes. Subsequently, the cells were incubated with
348 γH2Ax-antibody (1:400 in 1% BSA) at 4°C, overnight. A fluorochrome-conjugated anti-rabbit
349 secondary antibody (4412, Cell Signaling Technology) was then incubated for 1 hour at room
350 temperature. ß-actin staining was followed using phalloidin (8953, Cell Signaling Technology)
351 incubated for 15 minutes at RT. Coverslips were mounted in ProLong Gold Antifade Reagent with
352 DAPI (8961, Cell Signaling Technology), overnight. Immunofluorescence images were captured
353 using a Confocal Laser Scanning Biological Microscope Olympus FV1000 Fluoview.
354 Quantification of γH2Ax fluorescent cells was computed using Fiji software.
355

356 **Measuring production of reactive oxygen species (ROS)**

357 Oxidative stress induces the production of reactive oxygen species (ROS) and reactive nitrogen
358 species (RNS) in cells. We employed the OxiSelect™ *In Vitro* ROS/RNS Assay Kit (Green
359 Fluorescence), from Cell Biolabs, to evaluate the level of oxidative damage induced upon UV
360 exposure, intra- and extra-cellularly, immediately after exposure, 20 minutes and 1 day after

361 treatment recovery. Briefly, primary MEFs and HFFs were irradiated in triplicates in a 6-well
362 plate, twice a day (acute exposure) and once every day for 3 consecutive days (chronic
363 exposure). PBS solutions were collected immediately after the last UV treatments. After every
364 treatment, the cells were washed with pre-warmed PBS and complete media was replenished for
365 the accounted waiting timepoints. Thereafter, media solutions were collected 20 minutes and 24
366 hours after treatment cessation. These solutions were used to assess extracellular ROS signals.
367 Cytosolic ROS production was evaluated after trypsinization of the cells, lysis of cellular
368 membrane with 0.5% TritonX-100 and centrifugation for 5 minutes at 10,000 rpm. Samples were
369 loaded into a 96 black well plate and fluorescence signals were recorded using the Infinite 200
370 Tecan *i*-control plate reader machine at 480 nm excitation / 530 nm emission. We compared
371 extracellular ROS production in chronic samples after 2 exposure sessions with extracellular
372 ROS production in chronic samples after 3 sessions (**Supplementary Figure 5*D*).**
373

374 **DNA extraction and whole-genome sequencing**

375 Genomic DNA from MEFs and HFFs was extracted using Qiagen DNeasy Blood & Tissue kit,
376 following manufacturer instructions. Quality and quantity of DNA was checked using NanoDrop
377 and Qubit instruments. Thirteen high-quality DNA samples (primary, control and exposed
378 samples) were sent to Novogene for whole-genome library preparation and whole-genome
379 sequencing in paired-end 150 base-pair run mode using Illumina HiSeq-XTen at 30x coverage.
380

381 **Identification of somatic mutations and analysis of mutational signatures**

382 FASTQ files were subjected to BWA-MEM alignment using GRCm38 and GRCh38 as reference
383 genomes for MEF and HFF, respectively. Ensemble variant calling of somatic mutations was

384 performed using three independent variant callers Mutect2[50], VarScan2[51], Strelka2[52]. Any
385 mutation identified by at least two out of the three variant callers was considered a *bona fide*
386 mutation. *Bona fide* mutations were subsequently filtered to remove any residual SNPs based on
387 annotation by variant effect predictor[53]. Further, any mutations shared between two or more
388 samples were removed as these reflect either residual germline mutations or mutations under
389 positive selection. Finally, we collected *bona fide* mutations by removing clustered mutations in
390 each sample file. The remaining set of somatic mutations were used in the subsequent analyses
391 and evaluation for mutational signatures. Analysis of mutational signatures was performed using
392 our previously derived set of reference mutational signatures[33] as well as our previously
393 established methodology with the SigProfiler suite of tools used for summarization, simulation,
394 visualization, and extraction of mutational signatures[54-56].
395
396 **Additional visualization and analysis**
397 Variant allele frequency (VAF) data was generated using integrative genomics viewer[57]. R version
398 3.6.1 was used to plot data (*i.e.,* ggplot2, easyGgplot2, ComplexHeatmap[58], and circlize[59]
399 packages), to compute p-values (ggpur package), to perform correlation analyses (corrr package),
400 and to interrogate mutated cellular pathways (clusterProfiler[60] package).
401

FIGURE LEGENDS

Figure 1. Overview of the overall study design. Primary mammalian cells were expanded into 6-well plates and treated with ultraviolet light (UV) emitted from a UV-nail polish dryer for 20 minutes, twice a day within one single day, termed *acute UV exposure*. For *chronic UV exposure*, primary cells were exposed consecutively in three different days with each exposure lasting 20 minutes. Control samples were maintained in the dark in pre-warmed PBS for 20 minutes during each exposure session. *denotes to pre-mutagenic experimental assays performed on each condition, including interrogation of cytotoxicity, genotoxicity, and formation of reactive oxygen species. After recovery and cellular selection, whether through senescence bypass or single-cell subcloning, the cells emerged as clones and were subjected to DNA extraction, library preparation and whole-genome sequencing. Analysis of whole-genome sequenced samples was performed using our established pipelines for mutation calling. Analysis of mutational signatures was performed using the SigProfiler suite of tools.

Figure 2. Cytotoxicity and pre-mutagenic lesions in mammalian cells after irradiation by UV-nail dryer. ***(a)*** Cytotoxicity assessment following exposure of primary MEFs (left panel) and HFFs (right panel) to UV radiation emitted from the UV-nail polish dryer for different timepoints, ranging from 0 to 20 minutes. Multiple UV-exposure sessions were tested with one hour difference between each consecutive exposure, including: grey – one exposure; yellow – two exposures in a day; red – three exposures in a day. Absorbance was measured 48 hours after treatment cessation and was normalized to the control cells. The results are expressed as mean percentage ± SD (standard deviation) from at least three replicates. ***(b)*** DNA damage evaluation by immunofluorescence of Ser139-pjosphorylated histone H2Ax ((γH2Ax). Primary MEFs (top

425 panel) and HFFs (bottom panel) were exposed to UV radiation either acutely or chronically. ***(c)***
426 DNA damage quantification of γH2Ax-fluorescent cells represented as percentage to the total
427 number of counted cells, in MEFs and HFFs. ***(d)*** Accumulation of reactive oxygen species (ROS)
428 through time in primary MEFs (left panel) and HFFs (right panel) after acute and chronic exposure
429 to UV radiation. ROS formation, either cytosolic or extracellular, is represented as relative
430 fluorescence to the average fluorescence of the control cells. *: q-value≤0.05; **: q-value≤0.01;
431 ***: q-value≤0.001; ****:q-value≤0.0001.
432
433 **Figure 3. Mutations found in the genomes of mammalian cells irradiated by a UV-nail dryer.**
434 ***(a)*** Mutation count per megabase (Mb) detected in the different conditions, represented in colors,
435 in MEFs and HFFs (*: p-value<0.05). ***(b-c)*** Fold-increase of single base substitutions in UV-
436 treated clones compared to controls. Fold increase is expressed as mean fold-change ± SE
437 (standard error). ***(d-e)*** Spearman's correlations between the number of C>A substitutions and the
438 number UV exposures in UV-treated clones. Acute and chronic exposures correspond to 2 and 3
439 exposures, respectively. ***(f-g)*** Variant allelic frequency (VAF) analysis of single base substitutions.
440 Single base substitutions were binned in 3 windows, representing low VAF [0-0.33), medium VAF
441 [0.33-0.66) and high VAF [0.66-1] in UV-treated clones.
442
443 **Figure 4. Gene mutation analysis in UV-treated MEF and HFF clones.** ***(a-b)*** Non-synonymous
444 mutated genes respective to their VAF values. Red circles represent the mean VAF values. ***(c-d)***
445 VAF selected mutated genes, between 0.25 and 0.75, cross-referenced with the list from the
446 COSMIC Cancer Gene Census database. The color of each circles represents the corresponding
447 VAF value for each gene.

Figure 5. Mutational signatures imprinted by irradiating with a UV-nail polish dryer. ***(a)*** An example mutational pattern observed in one of the irradiated samples, *viz.,* MEF clone after chronic exposure with a UV-nail polish dryer. The pattern can be recapitulated (accuracy: 0.94) using the background mutation rate, as observed in respective spontaneous clones, and cosmic signature 18. Mutational signatures and mutational patterns are displayed using 96-plots. Single base substitutions are shown using the six subtypes of substitutions: C>A, C>G, C>T, T>A, T>C, and T>G. Underneath each subtype are 16 bars reflecting the sequence contexts determined by the four possible bases 5' and 3' to each mutated base. ***(b)*** Contributions of signature 18 across all examined samples. X-axis display the number of mutations attributed to signature 18 (log-scaled) while Y-axis reflects the accuracy for reconstructing the patterns of mutations observed in a samples using the background mutation rate and COSMIC signatures. Both spontaneous clones can be perfectly explained (accuracy: 1.00) as their pattern is the one used to create the background mutation rate.

SUPPLEMENTARY FIGURE LEGENDS

Supplementary Figure 1. Exposure and clonal expansion assays. ***(a)*** MEFs were treated at early passages and led through senescence manifested by a plateau-like curve where cells lost the ability to efficiently duplicate and grow. Cells can undergo senescence bypass and eventually emerge into immortalized clones, able to multiply indefinitely, a process called barrier-bypass clonal expansion, emulating carcinogenesis phenomenon. ***(b)*** HFFs were treated at early passages and led through recovery phase before initiating the single cell subcloning assay using serial dilutions technic. *Bona fide* single-cell clones were collected at the end of experiment.

Supplementary Figure 2. Schematic of whole-genome data analysis. Primary cells were sequenced and used as a germline reference. We employed three variant callers (Mutect2, VarScan2, and Strelka2) in matched tumor-normal mode, with the primary cells' BAM files as normal for each cell line. We selected variants called in at least 2 of the variant callers in order to increase variant calling quality. Germline single nucleotide polymorphisms (SNP) were removed using the dbSNP database. Any clustered mutation as well as any mutation observed in 2 or more samples were also removed. The final set of somatic mutations were analyzed by the SigProfiler suite of tools.

Supplementary Figure 3. Spearman correlations between numbers of substitutions and numbers of UV exposures in MEFs and HFFs. ***(a)*** Spearman correlations between numbers of single base substitutions and numbers of UV exposures in MEFs. ***(b)*** Spearman correlations between numbers of single base substitutions and numbers of UV exposures in HFFs.

Supplementary Figure 4. Analysis of variant allelic frequency analysis and small insertions and deletions. ***(a-b)*** Variant allelic frequency for *bona fide* mutations in MEF and HFF clones for each irradiation condition. ***(c)*** Number of small insertions and deletions (indels) in MEF and HFF clones for each irradiation condition.

Supplementary Figure 5. Toxicity and characteristics of the UV-nail polish dryer machine. ***(a)*** Intensity of UV radiation (mW/cm^2) at different position points (vertical and horizontal) in the UV nail polish dryer. ***(b)*** Stability over time of the intensity of UV radiation. ***(c)*** Cytotoxicity after repetitive UV exposure sessions in MEFs. 0 reflects control cells, 2 reflects acute exposure, and 3 reflects chronic exposure. Results are expressed as the mean value of three replicates ± SE (standard error). ***(d)*** Extracellular reactive oxygen species in MEFs exposed acutely (twice in one day) and chronically (2x: exposed once a day for 2 days; 3x: exposed once a day for 3 days).

Supplementary Table 1: Mutational signatures found in MEF and HFF clones. The background mutational pattern is based on the continuously ongoing clock-like mutational signatures and the mutational patterns observed in the spontaneous MEF and HFF clones. Numbers reflect the number of somatic mutations assigned to each signature. Accuracy is measured in cosine similarity between the original pattern of a sample and the pattern of a sample reconstructed using the assigned mutational signatures.

ACKNOWLEDGEMENTS

The authors would like to thank Dr. John Murray (Indiana University Bloomington) for providing human foreskin fibroblasts. This work was supported by Alfred P. Sloan Research Fellowship. LBA is also an Abeloff V scholar and he is personally supported by a Packard Fellowship for Science and Engineering. The funders had no roles in study design, data collection and analysis, decision to publish, or preparation of the manuscript.

AUTHOR CONTRIBUTIONS

LBA and MZ designed all experiments. MZ performed all experiments with help from NV and YY. MZ performed all data analysis with help from JD and YH. The manuscript was written by LBA and MZ with input from all other authors. LBA supervised the overall project and writing of the manuscript. All authors read and approved the final manuscript.

COMPETING INTERESTS

All authors declare no competing interests.

DATA AVAILABILITY

All whole-genome sequencing data have been deposited to Sequence Read Archive (SRA) and can be downloaded using accession number: PRJNA667106.

REFERENCES

1 Khan, A. Q., Travers, J. B. & Kemp, M. G. Roles of UVA radiation and DNA damage responses in melanoma pathogenesis. *Environ Mol Mutagen* **59**, 438-460, doi:10.1002/em.22176 (2018).

2 You, Y. H., Szabó, P. E. & Pfeifer, G. P. Cyclobutane pyrimidine dimers form preferentially at the major p53 mutational hotspot in UVB-induced mouse skin tumors. *Carcinogenesis* **21**, 2113-2117, doi:10.1093/carcin/21.11.2113 (2000).

3 Brem, R., Li, F. & Karran, P. Reactive oxygen species generated by thiopurine/UVA cause irreparable transcription-blocking DNA lesions. *Nucleic Acids Res* **37**, 1951-1961, doi:10.1093/nar/gkp070 (2009).

4 El Ghissassi, F. *et al.* A review of human carcinogens--part D: radiation. *Lancet Oncol* **10**, 751-752, doi:10.1016/s1470-2045(09)70213-x (2009).

5 cancer, I. A. f. R. o. C. W. G. o. a. u. U. l. a. s. The association of use of sunbeds with cutaneous malignant melanoma and other skin cancers: A systematic review. *Int J Cancer* **120**, 1116-1122, doi:10.1002/ijc.22453 (2007).

6 van Weelden, H., de Gruijl, F. R., van der Putte, S. C., Toonstra, J. & van der Leun, J. C. The carcinogenic risks of modern tanning equipment: is UV-A safer than UV-B? *Arch Dermatol Res* **280**, 300-307, doi:10.1007/bf00440604 (1988).

7 van Weelden, H., van der Putte, S. C., Toonstra, J. & van der Leun, J. C. UVA-induced tumours in pigmented hairless mice and the carcinogenic risks of tanning with UVA. *Arch Dermatol Res* **282**, 289-294, doi:10.1007/bf00375721 (1990).

8 Sterenborg, H. J. & van der Leun, J. C. Tumorigenesis by a long wavelength UV-A source. *Photochem Photobiol* **51**, 325-330, doi:10.1111/j.1751-1097.1990.tb01718.x (1990).

9 Kelfkens, G., de Gruijl, F. R. & van der Leun, J. C. Tumorigenesis by short-wave ultraviolet A: papillomas versus squamous cell carcinomas. *Carcinogenesis* **12**, 1377-1382, doi:10.1093/carcin/12.8.1377 (1991).

10 Greinert, R. *et al.* UVA-induced DNA double-strand breaks result from the repair of clustered oxidative DNA damages. *Nucleic Acids Res* **40**, 10263-10273, doi:10.1093/nar/gks824 (2012).

11 Didier, C., Emonet-Piccardi, N., Béani, J. C., Cadet, J. & Richard, M. J. L-arginine increases UVA cytotoxicity in irradiated human keratinocyte cell line: potential role of nitric oxide. *FASEB J* **13**, 1817-1824, doi:10.1096/fasebj.13.13.1817 (1999).

12 Francis, A. J. & Giannelli, F. Cooperation between human cells sensitive to UVA radiations: a clue to the mechanism of cellular hypersensitivity associated with different clinical conditions. *Exp Cell Res* **195**, 47-52, doi:10.1016/0014-4827(91)90498-j (1991).

13 Eisenstark, A. Mutagenic and lethal effects of near-ultraviolet radiation (290-400 nm) on bacteria and phage. *Environ Mol Mutagen* **10**, 317-337, doi:10.1002/em.2850100311 (1987).

14 Ridley, A. J., Whiteside, J. R., McMillan, T. J. & Allinson, S. L. Cellular and sub-cellular responses to UVA in relation to carcinogenesis. *Int J Radiat Biol* **85**, 177-195, doi:10.1080/09553000902740150 (2009).

15 Besaratinia, A., Bates, S. E., Synold, T. W. & Pfeifer, G. P. Similar mutagenicity of photoactivated porphyrins and ultraviolet A radiation in mouse embryonic fibroblasts: involvement of oxidative DNA lesions in mutagenesis. *Biochemistry* **43**, 15557-15566, doi:10.1021/bi048717c (2004).

16 Besaratinia, A., Kim, S. I., Bates, S. E. & Pfeifer, G. P. Riboflavin activated by ultraviolet A1 irradiation induces oxidative DNA damage-mediated mutations inhibited by vitamin C. *Proc Natl Acad Sci U S A* **104**, 5953-5958, doi:10.1073/pnas.0610534104 (2007).

17 Kim, S. I., Pfeifer, G. P. & Besaratinia, A. Mutagenicity of ultraviolet A radiation in the lacI transgene in Big Blue mouse embryonic fibroblasts. *Mutat Res* **617**, 71-78, doi:10.1016/j.mrfmmm.2006.12.003 (2007).

18 Pfeifer, G. P., You, Y. H. & Besaratinia, A. Mutations induced by ultraviolet light. *Mutat Res* **571**, 19-31, doi:10.1016/j.mrfmmm.2004.06.057 (2005).

19 Rieder, E. A. & Tosti, A. Cosmetically Induced Disorders of the Nail with Update on Contemporary Nail Manicures. *J Clin Aesthet Dermatol* **9**, 39-44 (2016).

20 Bollard, S. M. *et al.* Skin cancer risk and the use of UV nail lamps. *Australas J Dermatol* **59**, 348-349, doi:10.1111/ajd.12806 (2018).

21 Shipp, L. R., Warner, C. A., Rueggeberg, F. A. & Davis, L. S. Further investigation into the risk of skin cancer associated with the use of UV nail lamps. *JAMA Dermatol* **150**, 775-776, doi:10.1001/jamadermatol.2013.8740 (2014).

22 Ratycz, M. C., Lender, J. A. & Gottwald, L. D. Multiple Dorsal Hand Actinic Keratoses and Squamous Cell Carcinomas: A Unique Presentation following Extensive UV Nail Lamp Use. *Case Rep Dermatol* **11**, 286-291, doi:10.1159/000503273 (2019).

23 Ceballos, D. M. *et al.* Biological and environmental exposure monitoring of volatile organic compounds among nail technicians in the Greater Boston area. *Indoor Air* **29**, 539-550, doi:10.1111/ina.12564 (2019).

24 MacFarlane, D. F. & Alonso, C. A. Occurrence of nonmelanoma skin cancers on the hands after UV nail light exposure. *Arch Dermatol* **145**, 447-449, doi:10.1001/archdermatol.2008.622 (2009).

25 Viel, A. *et al.* A Specific Mutational Signature Associated with DNA 8-Oxoguanine Persistence in MUTYH-defective Colorectal Cancer. *EBioMedicine* **20**, 39-49, doi:10.1016/j.ebiom.2017.04.022 (2017).

26 Pilati, C. *et al.* Mutational signature analysis identifies MUTYH deficiency in colorectal cancers and adrenocortical carcinomas. *J Pathol* **242**, 10-15, doi:10.1002/path.4880 (2017).

27 Korenjak, M. & Zavadil, J. Experimental identification of cancer driver alterations in the era of pan-cancer genomics. *Cancer Sci* **110**, 3622-3629, doi:10.1111/cas.14210 (2019).

28 Bailey, M. H. *et al.* Comprehensive Characterization of Cancer Driver Genes and Mutations. *Cell* **174**, 1034-1035, doi:10.1016/j.cell.2018.07.034 (2018).

29 Gonzalez-Perez, A., Jene-Sanz, A. & Lopez-Bigas, N. The mutational landscape of chromatin regulatory factors across 4,623 tumor samples. *Genome Biol* **14**, r106, doi:10.1186/gb-2013-14-9-r106 (2013).

30 Plass, C. *et al.* Mutations in regulators of the epigenome and their connections to global chromatin patterns in cancer. *Nat Rev Genet* **14**, 765-780, doi:10.1038/nrg3554 (2013).

31 Youn, A. *et al.* A pan-cancer analysis of driver gene mutations, DNA methylation and gene expressions reveals that chromatin remodeling is a major mechanism inducing global changes in cancer epigenomes. *BMC Med Genomics* **11**, 98, doi:10.1186/s12920-018-0425-z (2018).

32 Tate, J. G. *et al.* COSMIC: the Catalogue Of Somatic Mutations In Cancer. *Nucleic Acids Res* **47**, D941-D947, doi:10.1093/nar/gky1015 (2019).

33 Alexandrov, L. B. *et al.* Signatures of mutational processes in human cancer. *Nature* **500**, 415-421, doi:10.1038/nature12477 (2013).

34 Alexandrov, L. B. & Stratton, M. R. Mutational signatures: the patterns of somatic mutations hidden in cancer genomes. *Curr Opin Genet Dev* **24**, 52-60, doi:10.1016/j.gde.2013.11.014 (2014).

35 Alexandrov, L. B. & Zhivagui, M. in *Encyclopedia of Cancer* 499-510 (2019).

36 Alexandrov, L. B. *et al.* Clock-like mutational processes in human somatic cells. *Nat Genet* **47**, 1402-1407, doi:10.1038/ng.3441 (2015).

37 Consortium, I. T. P.-C. A. o. W. G. Pan-cancer analysis of whole genomes. *Nature* **578**, 82-93, doi:10.1038/s41586-020-1969-6 (2020).

38 Alexandrov, L. B. *et al.* The repertoire of mutational signatures in human cancer. *Nature* **578**, 94-101, doi:10.1038/s41586-020-1943-3 (2020).

39 Zhivagui, M., Korenjak, M. & Zavadil, J. Modelling Mutation Spectra of Human Carcinogens Using Experimental Systems. *Basic Clin Pharmacol Toxicol* **121 Suppl 3**, 16-22, doi:10.1111/bcpt.12690 (2017).

40 Trucco, L. D. *et al.* Ultraviolet radiation-induced DNA damage is prognostic for outcome in melanoma. *Nat Med* **25**, 221-224, doi:10.1038/s41591-018-0265-6 (2019).

41 Moreno, N. C. *et al.* Whole-exome sequencing reveals the impact of UVA light mutagenesis in xeroderma pigmentosum variant human cells. *Nucleic Acids Res* **48**, 1941-1953, doi:10.1093/nar/gkz1182 (2020).

42 Feigelson, H. S. *et al.* Melanoma incidence, recurrence, and mortality in an integrated healthcare system: A retrospective cohort study. *Cancer Med* **8**, 4508-4516, doi:10.1002/cam4.2252 (2019).

43 Ferlay, J. *et al.* Estimating the global cancer incidence and mortality in 2018: GLOBOCAN sources and methods. *Int J Cancer* **144**, 1941-1953, doi:10.1002/ijc.31937 (2019).

44 Weir, H. K. *et al.* Melanoma in adolescents and young adults (ages 15-39 years): United States, 1999-2006. *J Am Acad Dermatol* **65**, S38-49, doi:10.1016/j.jaad.2011.04.038 (2011).

45 Tomasetti, C., Li, L. & Vogelstein, B. Stem cell divisions, somatic mutations, cancer etiology, and cancer prevention. *Science* **355**, 1330-1334, doi:10.1126/science.aaf9011 (2017).

46 Tomasetti, C., Marchionni, L., Nowak, M. A., Parmigiani, G. & Vogelstein, B. Only three driver gene mutations are required for the development of lung and colorectal cancers. *Proc Natl Acad Sci U S A* **112**, 118-123, doi:10.1073/pnas.1421839112 (2015).

47 Balmain, A. The critical roles of somatic mutations and environmental tumor-promoting agents in cancer risk. *Nat Genet* **52**, 1139-1143, doi:10.1038/s41588-020-00727-5 (2020).

48 Zhang, M. *et al.* Use of tanning beds and incidence of skin cancer. *J Clin Oncol* **30**, 1588-1593, doi:10.1200/JCO.2011.39.3652 (2012).

49 O'Sullivan, N. A. & Tait, C. P. Tanning bed and nail lamp use and the risk of cutaneous malignancy: a review of the literature. *Australas J Dermatol* **55**, 99-106, doi:10.1111/ajd.12145 (2014).

50 Benjamin, D. *et al.* Calling Somatic SNVs and Indels with Mutect2. *BioRxiv*, doi:10.1101/861054 (2019).

51 Koboldt, D. C. *et al.* VarScan 2: somatic mutation and copy number alteration discovery in cancer by exome sequencing. *Genome Res* **22**, 568-576, doi:10.1101/gr.129684.111 (2012).

52 Kim, S. *et al.* Strelka2: fast and accurate calling of germline and somatic variants. *Nat Methods* **15**, 591-594, doi:10.1038/s41592-018-0051-x (2018).

53 McLaren, W. *et al.* The Ensembl Variant Effect Predictor. *Genome Biol* **17**, 122, doi:10.1186/s13059-016-0974-4 (2016).

54 Bergstrom, E. N. *et al.* SigProfilerMatrixGenerator: a tool for visualizing and exploring patterns of small mutational events. *BMC Genomics* **20**, 685, doi:10.1186/s12864-019-6041-2 (2019).

55 Islam, S. M. A. *et al.* Uncovering novel mutational signatures by de novo extraction with SigProfilerExtractor. *bioRxiv*, 2020.2012.2013.422570, doi:10.1101/2020.12.13.422570 (2020).

56 Bergstrom, E. N., Barnes, M., Martincorena, I. & Alexandrov, L. B. Generating realistic null hypothesis of cancer mutational landscapes using SigProfilerSimulator. *BMC Bioinformatics* **21**, 438, doi:10.1186/s12859-020-03772-3 (2020).

57 Thorvaldsdóttir, H., Robinson, J. T. & Mesirov, J. P. Integrative Genomics Viewer (IGV): high-performance genomics data visualization and exploration. *Brief Bioinform* **14**, 178-192, doi:10.1093/bib/bbs017 (2013).

58 Gu, Z., Eils, R. & Schlesner, M. Complex heatmaps reveal patterns and correlations in multidimensional genomic data. *Bioinformatics* **32**, 2847-2849, doi:10.1093/bioinformatics/btw313 (2016).

59 Gu, Z., Gu, L., Eils, R., Schlesner, M. & Brors, B. circlize Implements and enhances circular visualization in R. *Bioinformatics* **30**, 2811-2812, doi:10.1093/bioinformatics/btu393 (2014).

60 Yu, G., Wang, L. G., Han, Y. & He, Q. Y. clusterProfiler: an R package for comparing biological themes among gene clusters. *OMICS* **16**, 284-287, doi:10.1089/omi.2011.0118 (2012).

Figure 1

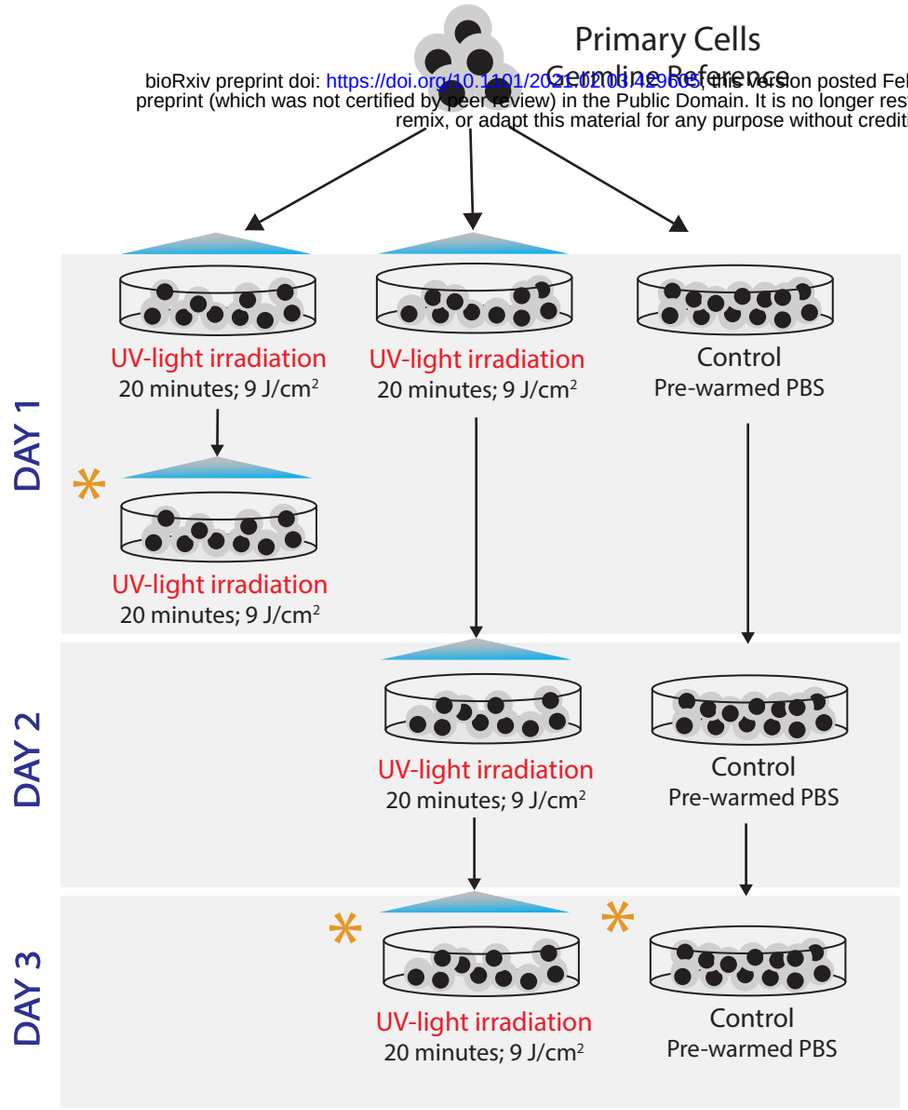

✳ Experimental assays:

Pre-mutagenic assessment	Assays	Time post-exposure
Oxidative damage	OxiSelect ROS/RNS Assay Kit	- Immediately - 20 minutes - 24 hours
DNA strand breaks	δH2Ax immuno-fluorescence	- 4 hours
Cytotoxicity	CCK-8 and trypan blue	- 48 hours

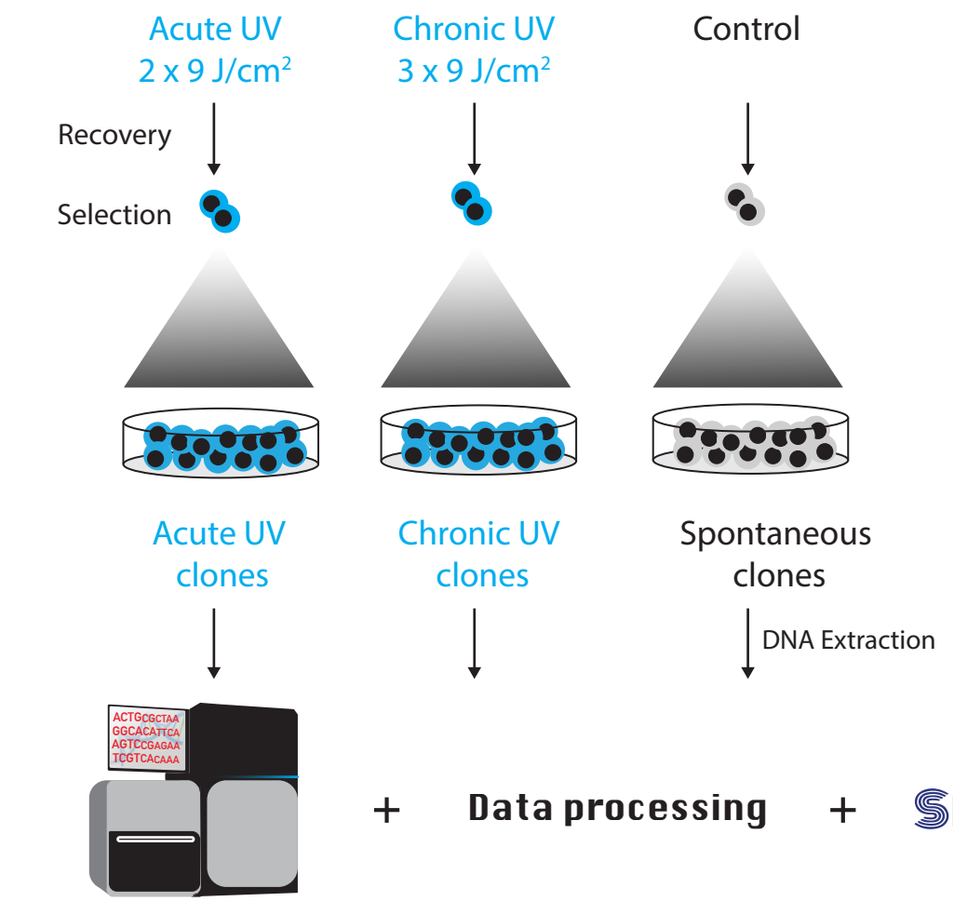

UV-light irradiation via UV-nail polish drying device

Exposed cells bottle-neck

Clonal expansion

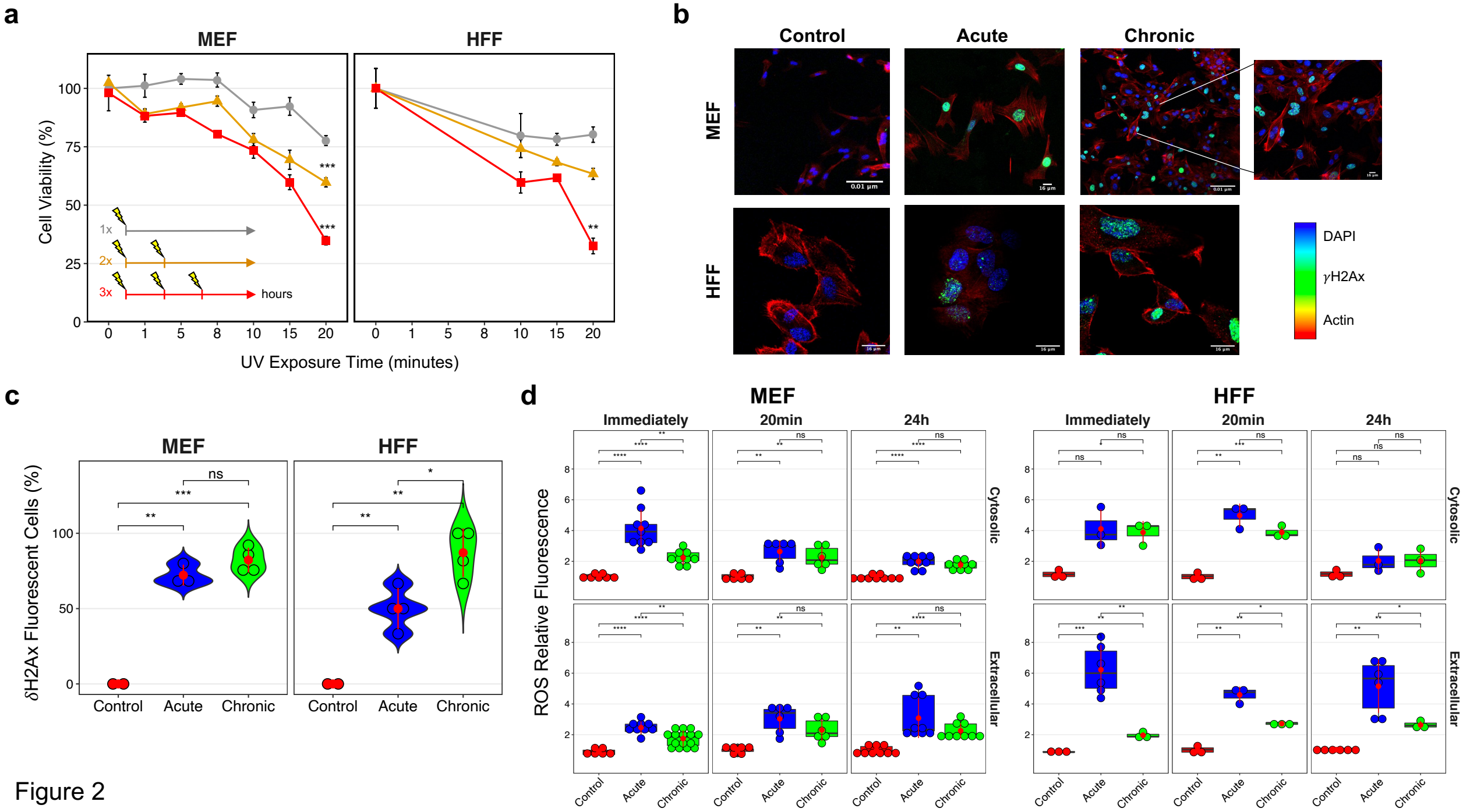
a
MEF
HFF
Cell Viability (%)
UV Exposure Time (minutes)
1x
2x
3x
hours
b
Control
Acute
Chronic
MEF
HFF
DAPI
γH2Ax
Actin
c
MEF
HFF
δH2Ax Fluorescent Cells (%)
Control
Acute
Chronic
d
MEF
HFF
Immediately
20min
24h
ROS Relative Fluorescence
Cytosolic
Extracellular

Figure 2

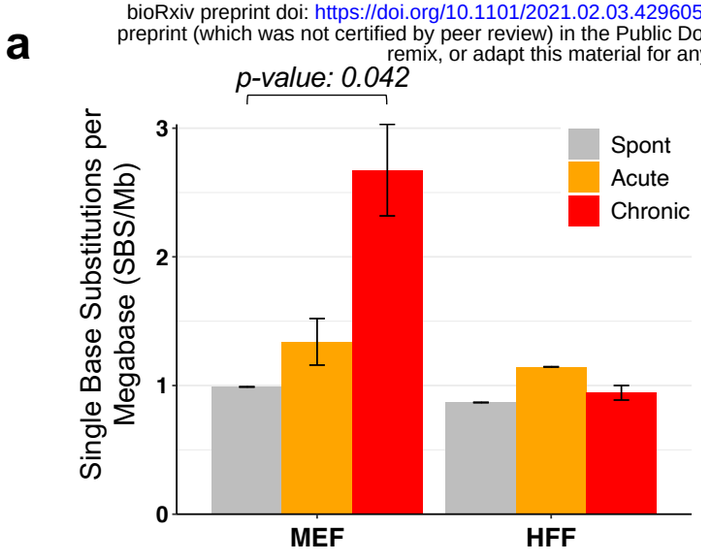

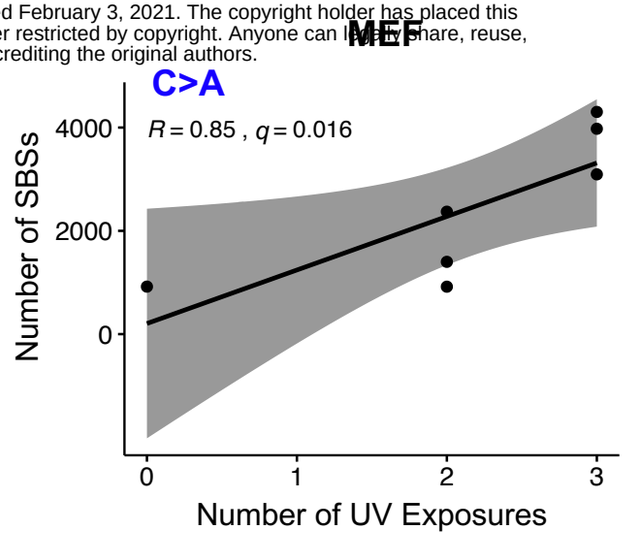

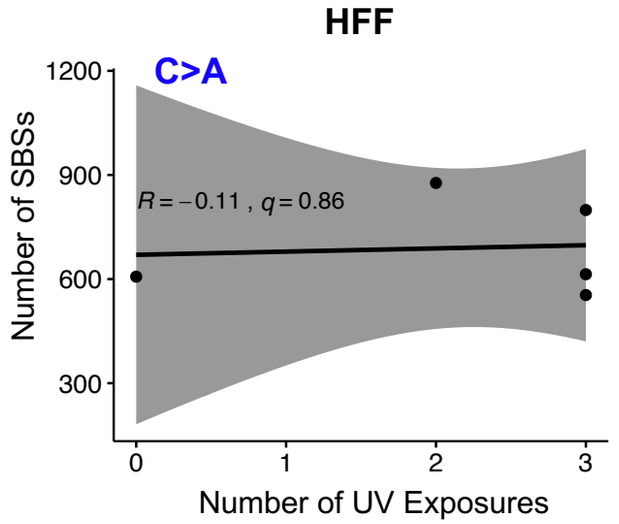

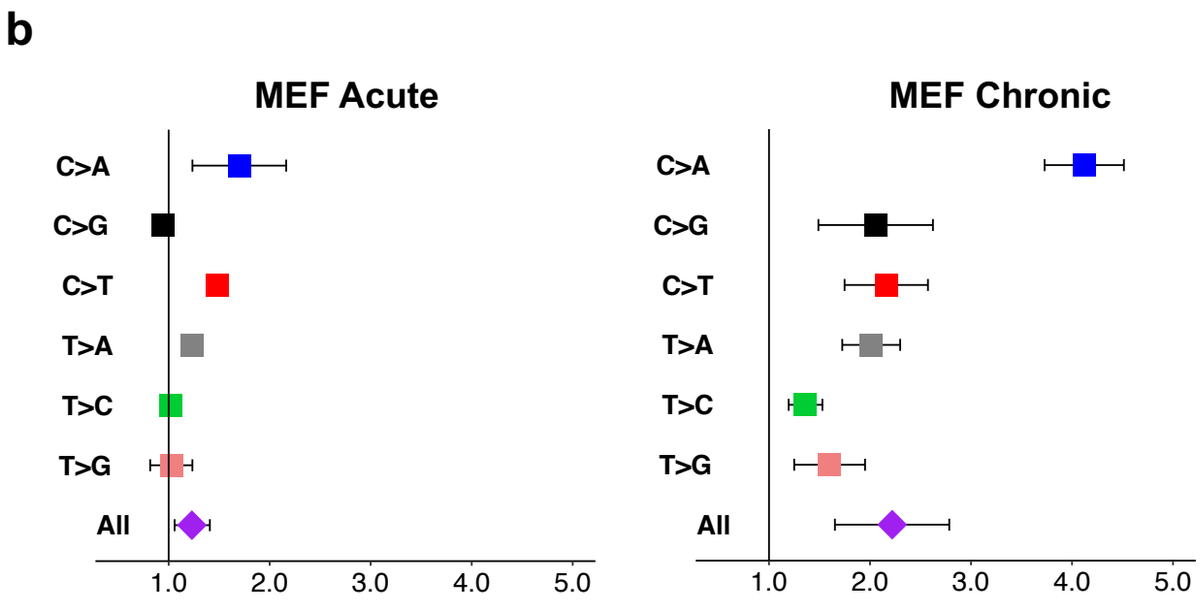

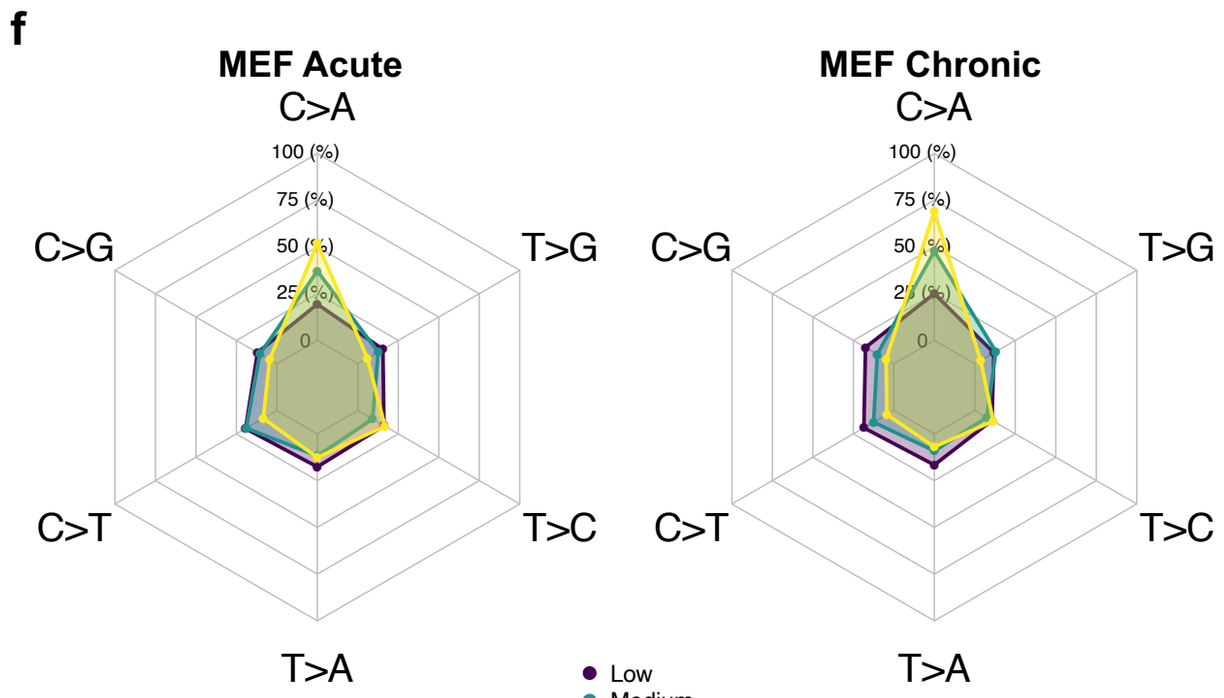

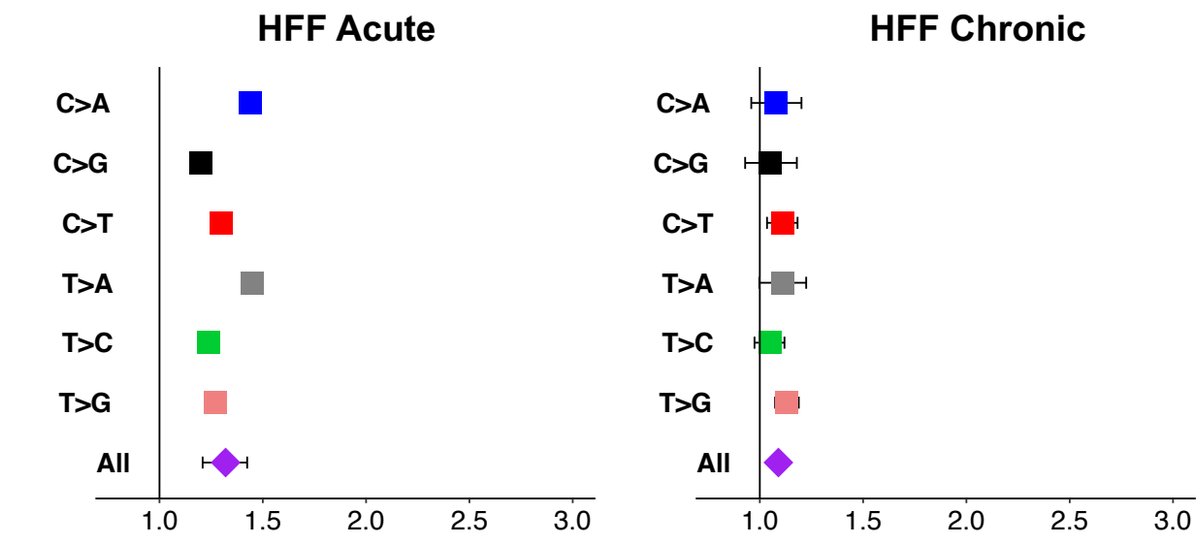

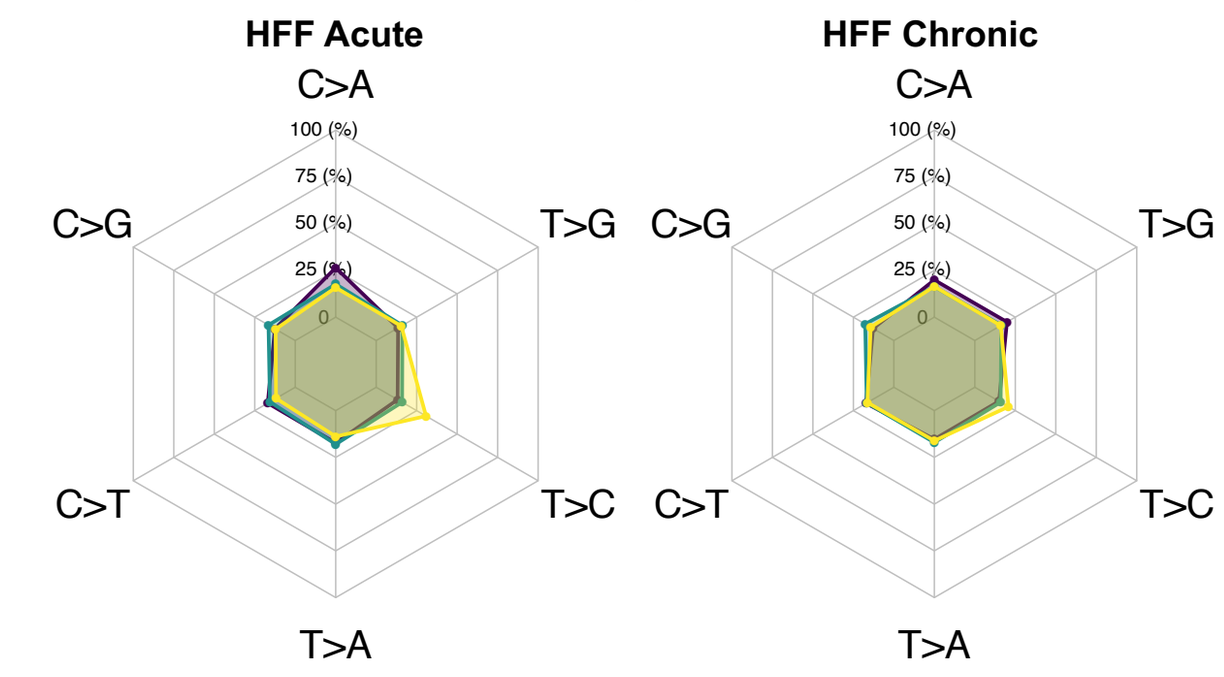

Figure 3

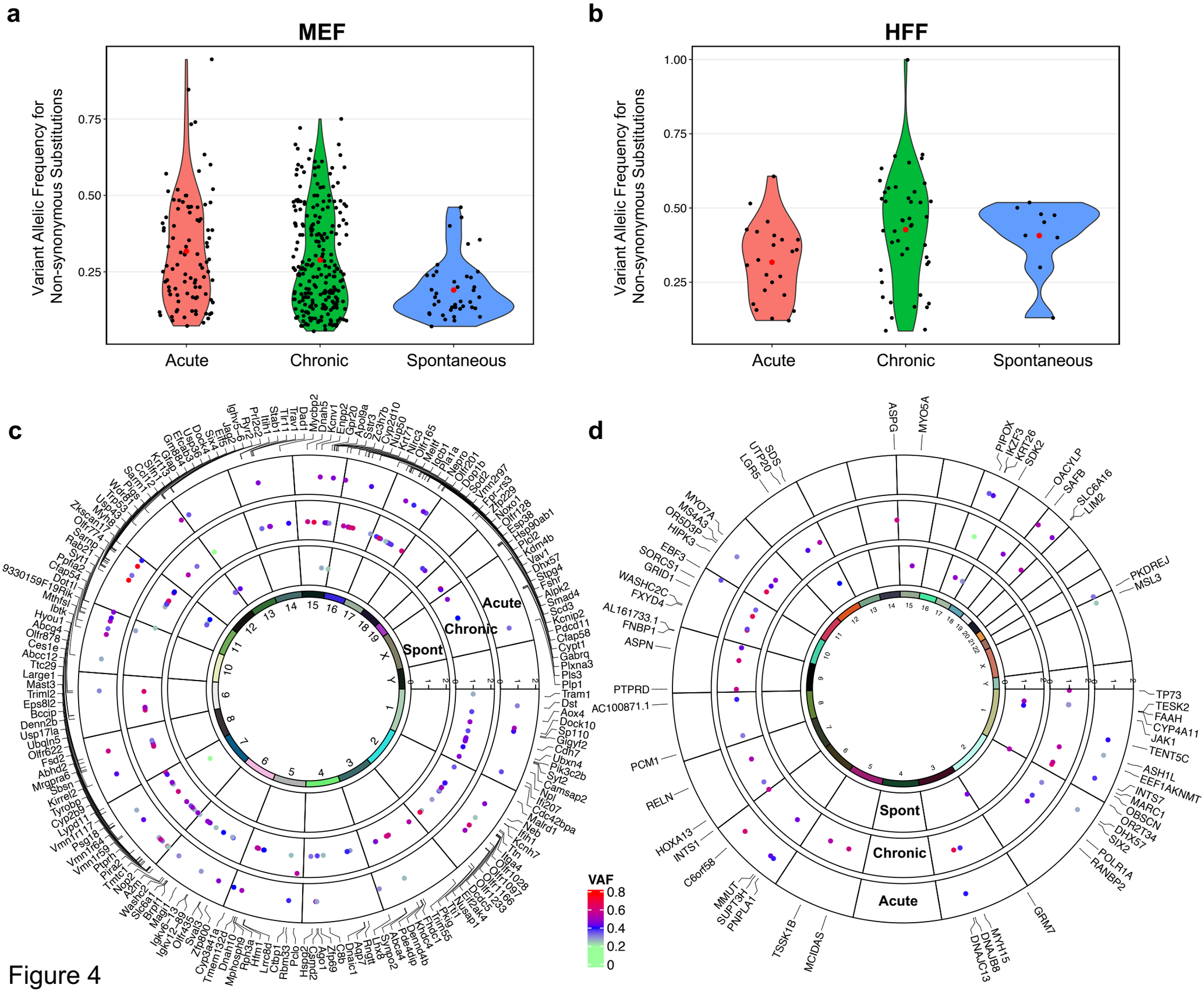
a
MEF
Variant Allelic Frequency for Non-synonymous Substitutions
0.75
0.50
0.25
Acute
Chronic
Spontaneous
b
HFF
Variant Allelic Frequency for Non-synonymous Substitutions
1.00
0.75
0.50
0.25
Acute
Chronic
Spontaneous
c
Acute
Chronic
Spont
d
Spont
Chronic
Acute
VAF
0.8
0.6
0.4
0.2
0

Figure 4

Figure 5

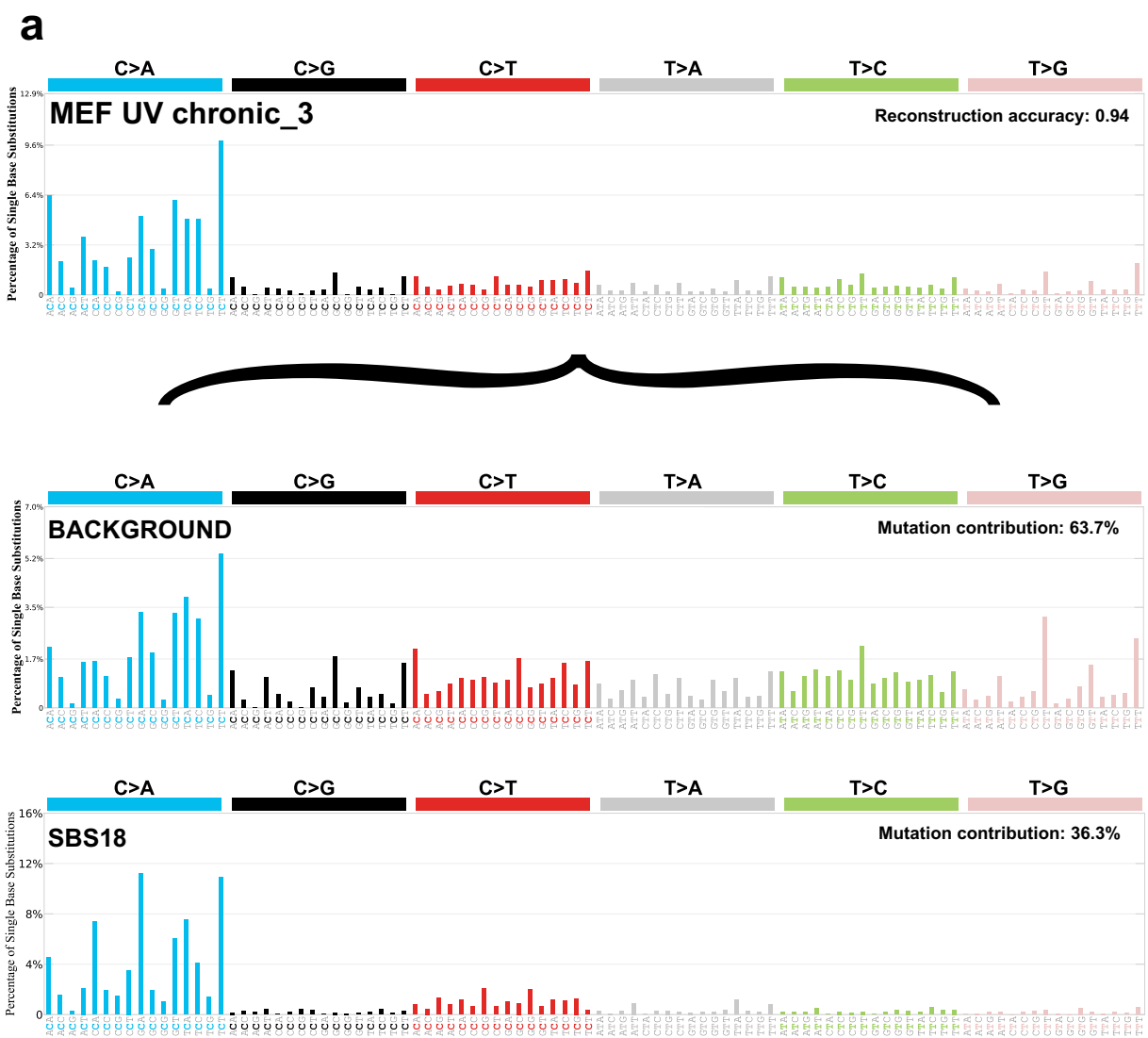
a
C>A
C>G
C>T
T>A
T>C
T>G
MEF UV chronic_3
Reconstruction accuracy: 0.94
Percentage of Single Base Substitutions
BACKGROUND
Mutation contribution: 63.7%
SBS18
Mutation contribution: 36.3%

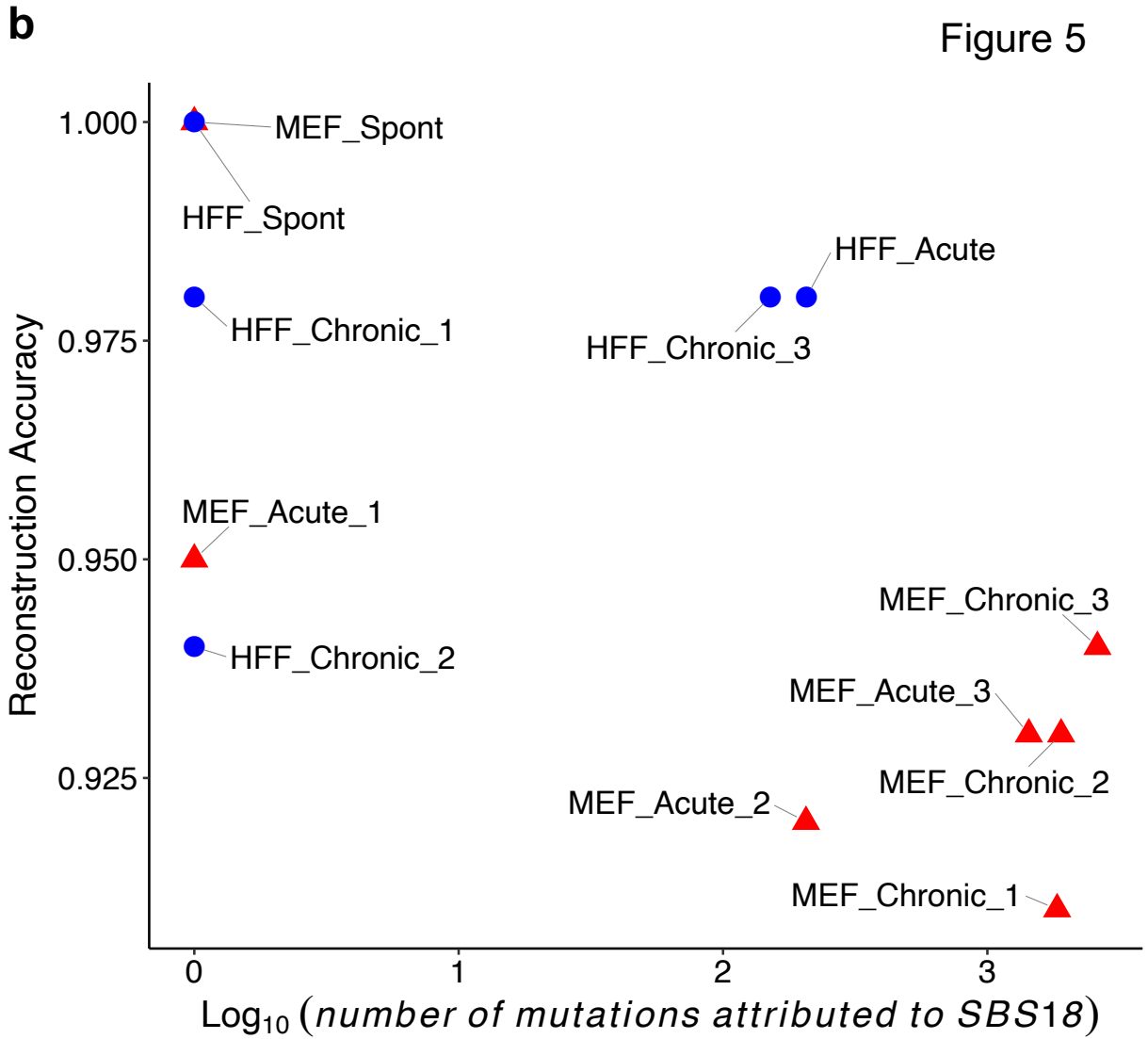
b
Reconstruction Accuracy
1.000
0.975
0.950
0.925
MEF_Spont
HFF_Spont
HFF_Chronic_1
HFF_Acute
HFF_Chronic_3
MEF_Acute_1
HFF_Chronic_2
MEF_Chronic_3
MEF_Acute_3
MEF_Chronic_2
MEF_Acute_2
MEF_Chronic_1
0
1
2
3
Log10 (number of mutations attributed to SBS18)